FOXM1 Participates in Scleral Remodeling in Myopia by Upregulating APOA1 Expression Through METTL3/YTHDF2

Min Xue,[1] Boai Li,[2,3] Yao Lu,[4,5] Luyuan Zhang,[6] Bing Yang,[7] and Lei Shi[1]

[1]Department of Ophthalmology, Anhui No. 2 Provincial People's Hospital/Anhui No. 2 Provincial People's Hospital Clinical College, Anhui Medical University/Anhui No. 2 Provincial People's Hospital Clinical College, Bengbu Medical University/Anhui Eye Hospital, Hefei, Anhui, China
[2]Dehong People's Hospital, The Affiliated Dehong Hospital of Kunming Medical University, Dehong, Yunan, China
[3]Clinical College of Ophthalmology, Tianjin Medical University, Tianjin Eye Institute, Tianjin Key Laboratory of Ophthalmology and Visual Science, Tianjin, China
[4]Graduate School of Bengbu Medical University, Bengbu, Anhui, China
[5]Department of Ophthalmology, Anhui No. 2 Provincial People's Hospital/Anhui Eye Hospital, Hefei, Anhui, China
[6]Tianjin Key Laboratory of Retinal Functions and Diseases, Tianjin Branch of National Clinical Research Center for Ocular Disease, Eye Institute and School of Optometry, Tianjin Medical University Eye Hospital, Tianjin, China
[7]School of Basic Medical Science, Tianjin Medical University, Tianjin, China

Correspondence: Lei Shi, Department of Ophthalmology, Anhui No. 2 Provincial People's Hospital/Anhui No. 2 Provincial People's Hospital Clinical College, Anhui Medical University/Anhui No. 2 Provincial People's Hospital Clinical College, Bengbu Medical University/Anhui Eye Hospital, Hefei, Anhui 233030, China; shileidr@outlook.com.

MX, BL, and YL contributed equally to the work presented here and should therefore be regarded as equivalent authors.

Received: June 29, 2023
Accepted: November 10, 2023
Published: January 8, 2024

Citation: Xue M, Li B, Lu Y, Zhang L, Yang B, Shi L. FOXM1 participates in scleral remodeling in myopia by upregulating APOA1 expression through METTL3/YTHDF2. *Invest Ophthalmol Vis Sci.* 2024;65(1):19. https://doi.org/10.1167/iovs.65.1.19

Purpose. Apolipoprotein A1 (*APOA1*) is a potential crucial protein and treatment goal for pathological myopia in humans. This study set out to discover the function of *APOA1* in scleral remodeling in myopia and its underlying mechanisms.

Methods. A myopic cell model was induced using hypoxia. Following loss- and gain-of function experiments, the expression of the myofibroblast transdifferentiation-related and collagen production-related factors Forkhead box M1 (*FOXM1*), *APOA1*, and methyltransferase-like 3 (*METTL3*) in the myopic cell model was examined by quantitative reverse transcription polymerase chain reaction (RT-qPCR) and western blotting. The proliferation and apoptosis were determined by Cell Counting Kit-8 assay and flow cytometry, respectively. Chromatin immunoprecipitation (ChIP) was employed to examine *FOXM1* enrichment in the *METTL3* promoter, methylated RNA immunoprecipitation (Me-RIP) to examine the N^6-methyladenosine (m^6A) modification level of *APOA1*, and photoactivatable ribonucleoside-enhanced crosslinking and immunoprecipitation (PAR-CLIP) to examine the binding between *METTL3* and *APOA1*.

Results. Hypoxia-induced human scleral fibroblasts (HSFs) had high *APOA1* and *FOXM1* expression and low *METTL3* expression. *FOXM1* knockdown elevated *METTL3* expression and downregulated *APOA1* expression. *FOXM1* was enriched in *METTL3* promoter. *APOA1* or *FOXM1* knockdown or *METTL3* overexpression reversed the hypoxia-induced elevation in vinculin, paxillin, and α-smooth muscle actin (α-SMA) levels and apoptosis and the reduction in collagen, type I, alpha 1 (COL1A1) level and cell proliferation in HSFs. *METTL3* or YTH N^6-methyladenosine RNA binding protein F2 (*YTHDF2*) knockdown or *APOA1* overexpression reversed the impacts of *FOXM1* knockdown on vinculin, paxillin, α-SMA, and COL1A1 expression and cell proliferation and apoptosis.

Conclusions. *FOXM1* elevated the m^6A methylation level of *APOA1* by repressing *METTL3* transcription and enhanced *APOA1* mRNA stability and transcription by reducing the *YTHDF2*-recognized m^6A methylated transcripts.

Keywords: myopia, forkhead box M1, methyltransferase-like 3, YTH domain family 2, apolipoprotein A1, scleral remodeling, hypoxia induction

Currently, myopia is characterized as a refractive abnormality of the non-accommodated eye that has a spherical equivalence of –0.5 diopters or less.[1] This disease occurs as a result of genetic and environmental risk factors.[2] Myopia is distinguished by increased axial length of the eye and invokes diverse complications, such as scleral/choroidal thinning, peripheral deformation, glaucoma, cataract, macular hole, myopic foveoschisis, retinal detachment, myopic choroidal neovascularization, and dome-shaped macula.[3] Considering the pathological complications and other related serious conditions of myopia, myopia is not only a negative factor for eye health, self-perception, and work/activity options but also a major contributor to blindness worldwide.[4] Because scleral remodeling leads to excessive elongation of the eye, which is the basis of myopia,[5] this study focuses on the molecular mechanisms

related to scleral remodeling in myopia, hoping to propose novel insights for the management of myopia.

Apolipoprotein A1 (*APOA1*) is the primary constituent of high-density lipoprotein and performs an essential function of reversing cholesterol transport.[6] *APOA1* exerts a role as a STOP signal through its ability to suppress excessive growth of the ocular axis.[7] A previous study indicated that *APOA1* is a potentially crucial protein and treatment target for pathological myopia in humans.[8] Wen et al.[9] indicated that the N^6-methyladenosine (m^6A) modifications have modulatory effects in the anterior capsule of the lens in patients with high myopia. SRAMP (sequence-based RNA adenosine methylation site predictor) database predictions indicate that *APOA1* has multiple m^6A modification sites, suggesting that *APOA1* might undergo m^6A modification in myopia. The m^6A modifications are modified by the m^6A methyltransferases (such as methyltransferase-like 3 [*METTL3*]), removed by the demethylases (such as fat mass and obesity-associated protein), and recognized by the m^6A binding proteins (e.g., YTH domain family 1, 2, and 3 [YTHDF1, YTHDF2, YTHDF3]).[10] Both *METTL3* and *YTHDF2* have been reported in ocular diseases. For example, *METTL3* affects angiogenesis in a hypoxia-induced retinopathy model.[11] Histone lactylation triggers the occurrence of ocular melanoma through promotion of *YTHDF2* expression.[12] Forkhead box M1 (*FOXM1*), a transcription factor of the Forkhead family, participates in normal cell proliferation.[13] Moreover, a prior study observed *FOXM1* expression in the entire ciliary marginal zone of the developing *Xenopus* retina,[14] suggesting that *FOXM1* might exert a critical influence on myopia.

Taken together, we speculated that *FOXM1* functions in myopia by modulating *METTL3*/*YTHDF2* to affect *APOA1* expression. Notably, Zhao et al.[15] reported that visual signals associated with myopia led to decreased permeability of choroidal capillaries and decreased blood flow. Reduced choroidal capillary permeability and blood flow led to reduced levels of oxygen and nutrient supply to the sclera, resulting in scleral hypoxia and ultimately excessive elongation of the ocular axis, suggesting scleral hypoxia as a control target for myopia.[16] Therefore, most of the cell models of myopia studied at present use hypoxia treatment of human scleral fibroblasts to simulate the myopia extracellular matrix (ECM) remodeling phenomenon.[16] Based on the previous data, we constructed a myopic cell model using hypoxia and then ascertained the function played by *FOXM1* in scleral remodeling of myopia through *APOA1* by orchestrating *METTL3*/*YTHDF2*.

Materials and Methods

Bioinformatics Analysis

The modification sites of *APOA1* m^6A were forecast using the SRAMP database (http://www.cuilab.cn/sramp). First, the GSE136701 dataset was downloaded through the Gene Expression Omnibus (GEO) database (http://www.ncbi.nlm.nih.gov/geo). Next, the differentially expressed genes of three patients with high myopia and three control patients with hyperopia were analyzed using the limma package for R (R Foundation for Statistical Computing, Vienna, Austria), with $|\log FC| > 1$ and $P < 0.05$ as screening criteria. The proteins interacted with were screened using the Starbase database (https://starbase.sysu.edu.cn/). The protein interaction was analyzed using the STRING database (https://cn.string-db.org/), and the results were plotted using CytoScape software. The datasets used or analyzed during the current study are available from the corresponding author on reasonable request.

Cell Culture and Treatment

Human scleral fibroblasts (HSFs; Procell, Wuhan, China) were cultivated with Gibco Dulbecco's Modified Eagle's Medium (Thermo Fisher Scientific, Waltham, MA, USA) encompassing 1% penicillin and streptomycin and 10% fetal bovine serum. After vimentin and keratin identification, HSFs at the fourth passage were adopted for the experiments. Cells were exposed to 21% O_2 as the normoxia (NO) group and to 5% O_2 as the hypoxia (HO) group. The medium was replenished on the second day of passaging. The cells were placed in a conventional CO_2 incubator (Heal Force, Shanghai, China) for 2, 4, 7, and 10 hours to determine the optimal time of hypoxic action. The cells received lysis for follow-up experiments after reaching the corresponding predetermined time.

Logarithmically growing HSFs underwent 0.25% trypsin digestion and dilution before being seeded into 96-well plates. When a 60% to 70% confluence was achieved, the cells were transfected or cotransfected with lentivirus (LV)-*METTL3*, LV-*APOA1*, LV-negative control (NC), small interfering RNA (si)-*APOA1*, si-*FOXM1*, si-*YTHDF1*, si-*YTHDF2*, and si-NC plasmids (75 nM; GenePharma, Shanghai, China) following the directions for the Invitrogen Lipofectamine 3000 Transfection Reagent (Thermo Fisher Scientific). Subsequently, the transfected cells were subjected to the appropriate normoxic or hypoxic treatment for subsequent experimentations. The cells were classified as follows: NO (normoxia-treated HSFs), HO (hypoxia-treated HSFs), NO+NC (normoxia-treated HSFs transfected with si-NC), NO+si-APOA1 (normoxia-treated HSFs transfected with si-*APOA1*), NO+si-FOXM1 (normoxia-treated HSFs transfected with si-*FOXM1*), HO+NC (hypoxia-treated HSFs transfected with si-NC), HO+si-*APOA1* (hypoxia-treated HSFs transfected with si-*APOA1*), HO+si-*FOXM1* (hypoxia-treated HSFs transfected with si-*FOXM1*), NO+LV-NC (normoxia-treated HSFs transfected with LV-NC), NO+LV-*METTL3* (normoxia-treated HSFs transfected with LV-*METTL3*), HO+LV-NC (hypoxia-treated HSFs transfected with LV-NC), HO+LV-*METTL3* (hypoxia-treated HSFs transfected with LV-*METTL3*), HO+si-FOXM1+si-METTL3 (hypoxia-treated HSFs cotransfected with si-*FOXM1* and si-*METTL3*), HO+si-FOXM1+LV-APOA1 (hypoxia-treated HSFs cotransfected with si-*FOXM1* and LV-*APOA1*), or HO+si-FOXM1+si-YTHDF2 (hypoxia-treated HSFs cotransfected with si-*FOXM1* and si-*YTHDF2*). The knockdown plasmid sequences are listed in Supplementary Table S1.

Western Blotting

Total proteins were derived from the cells using the radioimmunoprecipitation assay lysis solution encompassing phenylmethylsulfonyl fluoride (PMSF). Following 30-minute incubation on ice, the proteins were centrifuged at 4°C and 8000*g* for 10 minutes to attain the supernatant. A bicinchoninic acid kit was applied for measuring the protein concentration. Then, the proteins (50 µg) were dissolved in 2× sodium dodecyl sulfate (SDS) loading buffer, boiled for 5 minutes at 100°C, and subjected to SDS–polyacrylamide

Investigative Ophthalmology & Visual Science

gel electrophoresis (SDS-PAGE). After the proteins were transferred to polyvinylidene fluoride membranes by the wet transfer method, 5% skimmed-milk powder was employed to block the membranes at room temperature for 1 hour. The membranes then underwent overnight incubation with diluted primary antibodies (Abcam, Cambridge, UK) against vinculin (ab219649, 1:1000), paxillin (ab32084, 1:1000), α-smooth muscle actin (α-SMA, ab7817, 1:1000), collagen, type I, alpha 1 (COL1A1, ab138492, 1:1000), YTHDF2 (ab220163, 1:1000), transforming growth factor-beta 1 (TGF-β1, ab215715, 1:1000), and alpha-tubulin (ab7291, 1:10,000) at 4°C. Subsequent to washing, the membranes received 2 hours of incubation with horseradish peroxidase–labeled secondary antibody immunoglobulin G (IgG, ab205718, 1:5000; Abcam) at room temperature and development with electrochemical luminescence. The membranes were scanned and analyzed on a gel imager, and the bands in the western blotting images were quantified in grayscale using Image J (National Institutes of Health, Bethesda, MD, USA) with alpha-tubulin as an internal reference.

Immunofluorescence Staining

Cells underwent 30 minutes of 4% paraformaldehyde fixation, phosphate-buffered saline with Tween 20 (PBST) washing, and 15 minutes of 0.5% Triton X-100 permeabilization. The cells then underwent 1 hour of blocking with 5% bovine serum albumin followed by overnight incubation with primary antibodies (1:200, Abcam) against vimentin (ab92547) and keratin (ab185627) at 4°C. Following PBST washing, the cells were subjected to 1 hour of incubation at room temperature with fluorescent secondary antibody and nuclei staining with 4′,6-diamidino-2-phenylindole. Following a PBST washing, the slides were sealed with fluorescent mounting medium for photography under a fluorescent microscope.

Quantitative Reverse Transcription Polymerase Chain Reaction

Total RNA was isolated from cells using TRIzol Reagent (Life Technologies, Carlsbad, CA, USA), with a NanoDrop 2000 ultra-micro spectrophotometer (Thermo Fisher Scientific) to determine RNA concentration and purity. The reverse transcription reaction was conducted in a PCR amplifier following the reverse transcription kit (11750150; Thermo Fisher Scientific) to synthesize cDNA templates. Specifically, 2 µg total RNA was added to a 0.5-mL microcentrifuge tube and supplemented with an appropriate amount of diethyl pyrocarbonate water to achieve a total volume of 11 µL. The tubes were filled with 10-µM Oligo(dT) Primer (12–18 µL) with gentle mixing and centrifugation. Following 10 minutes of heating at 70°C, the microcentrifuge tubes were immediately inserted into an ice bath for at least 1 minute followed by the addition of 10× PCR buffer, 25-mM MgCl, 10-mM dNTP mix, and 0.1-M dithiothreitol to form a 50-µL system, followed by gentle mixing, centrifugation, and 2 to 5 minutes of incubation at 42°C. The tubes were supplemented with 1 µL Invitrogen SuperScript II Reverse Transcriptase, incubated at 42°C for 50 minutes, and heated at 70°C for 15 minutes to terminate the reaction. The tubes were then inserted into ice, 1 µL RNase H was added, and the tubes were incubated for 20 minutes at 37°C to degrade the residual RNA. Real-time quantitative reverse transcription polymerase chain reaction (RT-qPCR) experiments were conducted following the instructions of the TransStart Green qPCR SuperMix kit (Transgen Biotech, Beijing, China) using a fluorescent qPCR analyzer (CFX Connect; Bio-Rad, Hercules, CA, USA), in which glyceraldehyde-3-phosphate dehydrogenase served as a normalizer for RNA expression. The reaction was pre-denatured for 10 minutes at 95°C and then denatured for 10 seconds at 95°C, annealed for 20 seconds at 60°C, and extended for 34 seconds at 72°C for 40 cycles. Data analysis was conducted using the $2^{-\Delta\Delta Ct}$ method.[17] The primer sequences are listed in the Table.

Table. Primer Sequences

Primer	Sequences (5′–3′)
FOXM1-F	TGGCAGAGTCCAACTCTTGCAAG
FOXM1-R	GGTTTGGGTTTGAGGCCGGAGTC
APOA1-F	CTTCCTGACGGGGAGCCAGGCTC
APOA1-R	GGTTATCCCAGAACTCCTGGGTC
METTL3-F	CTATCTCCTGGCACTCGCAAGA
METTL3-R	GCTTGAACCGTGCAACCACATC
YTHDF1-F	CAAGCACACAACCTCCATCTTCG
YTHDF1-R	GTAAGAAACTGGTTCGCCCTCAT
YTHDF2-F	TAGCCAGCTACAAGCACACCAC
YTHDF2-R	CAACCGTTGCTGCAGTCTGTGT
GAPDH-F	GTGGCTGGCTCAGAAAAAGG
GAPDH-R	GGGGAGATTCAGTGTGGTGG

F, forward; R, reverse.

Measurement of RNA Lifetime

The RNA stability assay was performed as previously described.[18] HSFs (1×10^5 cells) with 50% confluence were seeded onto 10-cm plates, followed by 24-hour incubation in a conventional CO_2 incubator. After that, the cells on a 10-cm plate were reseeded onto three 6-cm plates. After 48 hours, the cells were collected by trypsin digestion, and actinomycin D was added to the cells at a concentration of 5 mg/mL at 6 hours, 3 hours, and 0 hour. Total RNA was purified using the RNeasy Kit with DNase-I digestion procedures attached to the column. RT-qPCR was conducted to examine the RNA quantity.

Chromatin Immunoprecipitation

The EZ-ChIP kit (MilliporeSigma, Bedford, MA, USA) was utilized for chromatin immunoprecipitation (ChIP) assays. Cells were cultivated for 36 hours and fixed with formaldehyde, and the fixation was terminated using glycine. The cells were then scraped and centrifuged to obtain the cell precipitate. The precipitate was suspended with a cell lysis solution containing PMSF and centrifuged before the supernatant was discarded. After sonication in an ice-water bath to precipitate the DNA, 10% of the supernatant was taken as control and the remaining 90% of the lysate was incubated with anti-FOXM1 antibody (ab240753; Abcam) or normal rabbit IgG antibody (5946; Cell Signaling Technologies) coupled with magnetic beads and then centrifuged. DNA bound to FOXM1 protein was eluted with eluent and then purified using a DNA purification kit (Beyotime, Shanghai, China), followed by RT-qPCR.

Investigative Ophthalmology & Visual Science

Cell Counting Kit-8 Assay

HSFs were seeded onto 96-well plates with 100 µL diluted cell suspension (1×10^6 cells/mL) per well; there was a set of three replicates. Following 24 hours, 48 hours, or 72 hours of incubation in the incubator, each well of cells was incubated for 2 hours with 10 µL Cell Counting Kit-8 (CCK-8) reagent (Abcam) in the incubator. A microplate reader (BioTek Instruments, Winooski, VT, USA) was applied for measuring the absorbance value at 450 nm, and the average value of the three replicates was calculated with analysis of cell growth.

Flow Cytometry

Following 48 hours of transfection, cells were digested with EDTA-free 0.25% trypsin (YB15050057; YBio, Shanghai, China), collected in flow tubes, and centrifuged, and the supernatants were removed. Following three washes with cold PBS, the cells were centrifuged, and the supernatants were removed. This assay was conducted following the specifications of the Annexin V-FITC Apoptosis Kit Plus (K201-100; BioVision, Milpitas, CA, USA). The cells were resuspended in the staining solution, shaken, mixed, incubated at room temperature for 15 minutes, and shaken and mixed with 1 mL HEPES buffer solution (PB180325; Procell). Apoptosis was evaluated by flow cytometry.

Methylated RNA Immunoprecipitation

Total RNA was isolated from HSFs by the TRIzol method, and mRNA in the total RNA was isolated and purified using the PolyATtract mRNA Isolation System (A-Z5300; A&D Technology Corporation, Beijing, China). The immunoprecipitation (IP) buffer (2-mM EDTA; 140-mM NaCl; 20-mM Tris, pH 7.5; and 1% Nonidet P-40) was incubated for 1 hours with anti-m^{6}A antibodies (1:500, ab151230; Abcam) or anti-IgG antibodies (ab109489, 1:100; Abcam) and protein A/G magnetic beads for binding. The isolated and purified mRNA and magnetic bead-antibody complexes were added to the IP buffer encompassing ribonuclease and protease inhibitors for overnight reaction at 4°C. The RNA was eluted with elution buffer and purified using phenol–chloroform extraction, and RT-qPCR was employed for APOA1 analysis.[19,20] The primer sequences are listed in the Table.

Photoactivatable Ribonucleoside-Enhanced Crosslinking and Immunoprecipitation

HSFs underwent 14 hours of incubation with 200 mm 4-thiopyridine (Sigma-Aldrich, St. Louis, MO, USA) followed by cross-linking with 0.4 J/cm^2 at 365 nm. Following lysis, the cells were immunoprecipitated with METTL 3 antibodies (5 and 3 mg, respectively) at 4°C. The precipitated RNA was labeled with [γ-^{32}P]-adenosine triphosphate and visualized by radioautography. The photoactivatable ribonucleoside (PAR) fragments were digested by proteinase K to remove proteins, and RNA was isolated for qRT-PCR to examine APOA1 expression.

Statistical Analysis

Prism 8.0 (GraphPad, Boston, MA, USA) was utilized for the statistical analysis, and all data are stated as mean ± standard deviation (SD). Unless otherwise specified, *t*-tests were performed to compare data between two groups, and one-way ANOVA tests were performed to compare data among multiple groups with Tukey's multiple comparison tests. $P < 0.05$ was considered statistically significant.

Results

METTL3 Expression was Reduced in Hypoxia-Treated HSFs

Predictions of the m^{6}A modification sites of *APOA1* by the SRAMP database (http://www.cuilab.cn/sramp) indicated the presence of multiple m^{6}A modification sites on *APOA1* (Fig. 1A), suggesting that *APOA1* might experience m^{6}A modification in myopia. HSFs were treated with hypoxia to construct a myopic cell model. Immunofluorescence results indicated that the cultivated HSFs were positive for vimentin and negative for keratin (Fig. 1B), thus confirming that the cells were HSFs. After hypoxia treatment, myofibroblast transdifferentiation and collagen production in HSFs were examined using western blotting. The results indicated that protein expression of the focal adhesion proteins vinculin and paxillin and the myofibroblast marker α-SMA was considerably augmented, but COL1A1 protein expression was appreciably reduced in hypoxia-treated HSFs compared with the normoxia-treated cells (Fig. 1C), suggesting that the myopic cell model was successfully constructed using hypoxia. RT-qPCR results showed that *METTL3* expression was downregulated in hypoxia-treated HSFs as compared to normoxia-treated HSFs (Fig. 1D). Methylated RNA immunoprecipitation (Me-RIP) assay of the m^{6}A modification level of *APOA1* in HSFs revealed a considerable reduction in the m^{6}A modification level of *APOA1* in hypoxia-treated HSFs compared with normoxia-treated HSFs (Fig. 1E). The results of photoactivatable ribonucleoside-enhanced crosslinking and immunoprecipitation (PAR-CLIP) assays illustrated that, compared to normoxia treatment, hypoxia treatment resulted in a substantial decrease in *APOA1* expression pulled down by *METTL3* antibodies (Fig. 1F). These results indicate that *METTL3* mediated m^{6}A modification of *APOA1* in the hypoxia-induced myopic cell model.

YTHDF2 Increases *APOA1* Expression in Hypoxia-Treated HSFs

Next, we further examined whether *APOA1* influences scleral remodeling in myopia through m^{6}A methylation regulation. First, si-*APOA1* was transfected into HSFs, and RT-qPCR displayed a dramatic decrease in *APOA1* expression, suggesting that the system designed to interfere with *APOA1* expression was successfully constructed (Fig. 2A). Western blotting demonstrated that si-*APOA1* transfection markedly diminished vinculin, paxillin, and α-SMA protein levels and elevated COL1A1 protein levels in HSFs after hypoxia treatment (Fig. 2B). Moreover, LV-*METTL3* transfection also reversed the hypoxia-induced elevation in vinculin, paxillin, and α-SMA protein levels and reduction in COL1A1 protein levels in HSFs (Fig. 2C). RT-qPCR and western blotting showed that LV-*METTL3* transfection resulted in a pronounced reduction in *APOA1* expression in HSFs after hypoxia treatment (Figs. 2D, 2E).

To investigate whether m^{6}A-methylated *APOA1* is affected by *YTHDF1* or *YTHDF2*, HSFs were transfected with si-*YTHDF1* or si-*YTHDF2*. RT-qPCR and western

Investigative Ophthalmology & Visual Science

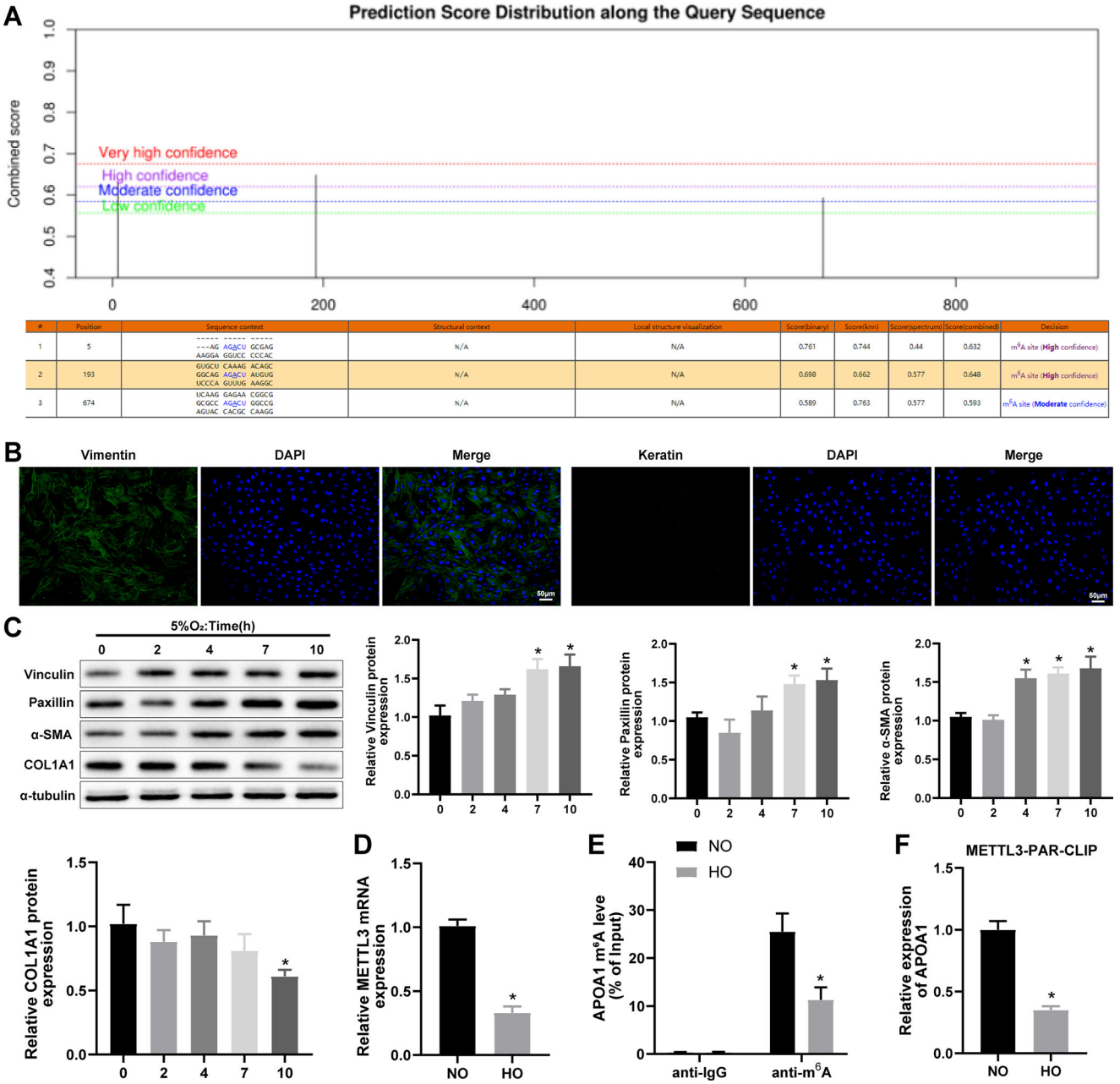

#	Position	Sequence context	Structural context	Local structure visualization	Score(binary)	Score(knn)	Score(spectrum)	Score(combined)	Decision
1	5	AGACU GCGAG / AAGGA GGUCC CCCAC	N/A	N/A	0.761	0.744	0.44	0.632	m6A site (High confidence)
2	193	GUGCU CAAAG ACAGC / GGCAG AGACU AUGUG / UCCCA GUUUG AAGGC	N/A	N/A	0.698	0.662	0.577	0.648	m6A site (High confidence)
3	674	UCAAG GAGAA CGGCG / GCGCC AGACU GGCCG / AGUAC CACGC CAAGG	N/A	N/A	0.589	0.763	0.577	0.593	m6A site (Moderate confidence)

Figure 1. Hypoxia treatment reduced *METTL3* levels in HSFs. (**A**) SRAMP database prediction of m^{6}A modification sites of *APOA1*. (**B**) Immunofluorescence evaluation of vimentin and keratin in HSFs. (**C**) Western blotting examination of myofibroblast transdifferentiation and collagen production in hypoxia-treated HSFs with one-way ANOVA to confirm *P* values and Tukey's multiple comparison tests. (**D**) RT-qPCR examination of mRNA expression of m^{6}A-related factor in hypoxia- and normoxia-treated HSFs. (**E**) Me-RIP examination of *APOA1* m^{6}A modification levels in hypoxia- and normoxia-treated HSFs. (**F**) PAR-CLIP examination of the binding between *METTL3* and *APOA1* mRNA. Unless otherwise stated, the *t*-test was applied to confirm the *P* values; $N = 3$.

blotting indicated that si-*YTHDF1* transfection did not affect *APOA1* expression, whereas si-*YTHDF2* transfection apparently enhanced *APOA1* mRNA and protein expression (Figs. 2F, 2G). The results of the PAR-CLIP experiment further confirmed the direct relationship between *YTHDF2* and *APOA1* (Fig. 2H). Moreover, si-*YTHDF2* transfection lowered the degradation rate of *APOA1* mRNA (Fig. 2I). These findings suggest that the reduction of m^{6}A-methylated *APOA1* transcripts recognized by *YTHDF2* slowed the *APOA1* degradation rate, thereby promoting *APOA1* expression in hypoxia-treated HSFs.

FOXM1 Indirectly Affects *APOA1* Expression by Downregulating *METTL3* Expression to Participate in Scleral Remodeling in Myopia

Differential gene expression microarrays in myopia were screened in the GEO database (https://www.ncbi.nlm.nih.gov/geo/), and the microarray GSE136701 was selected for differential gene analysis using the limma package in R. The proteins interacting with *YTHDF2* were screened by the Starbase database (https://starbase.sysu.edu.cn/) and intersected with the differentially expressed genes in GSE136701,

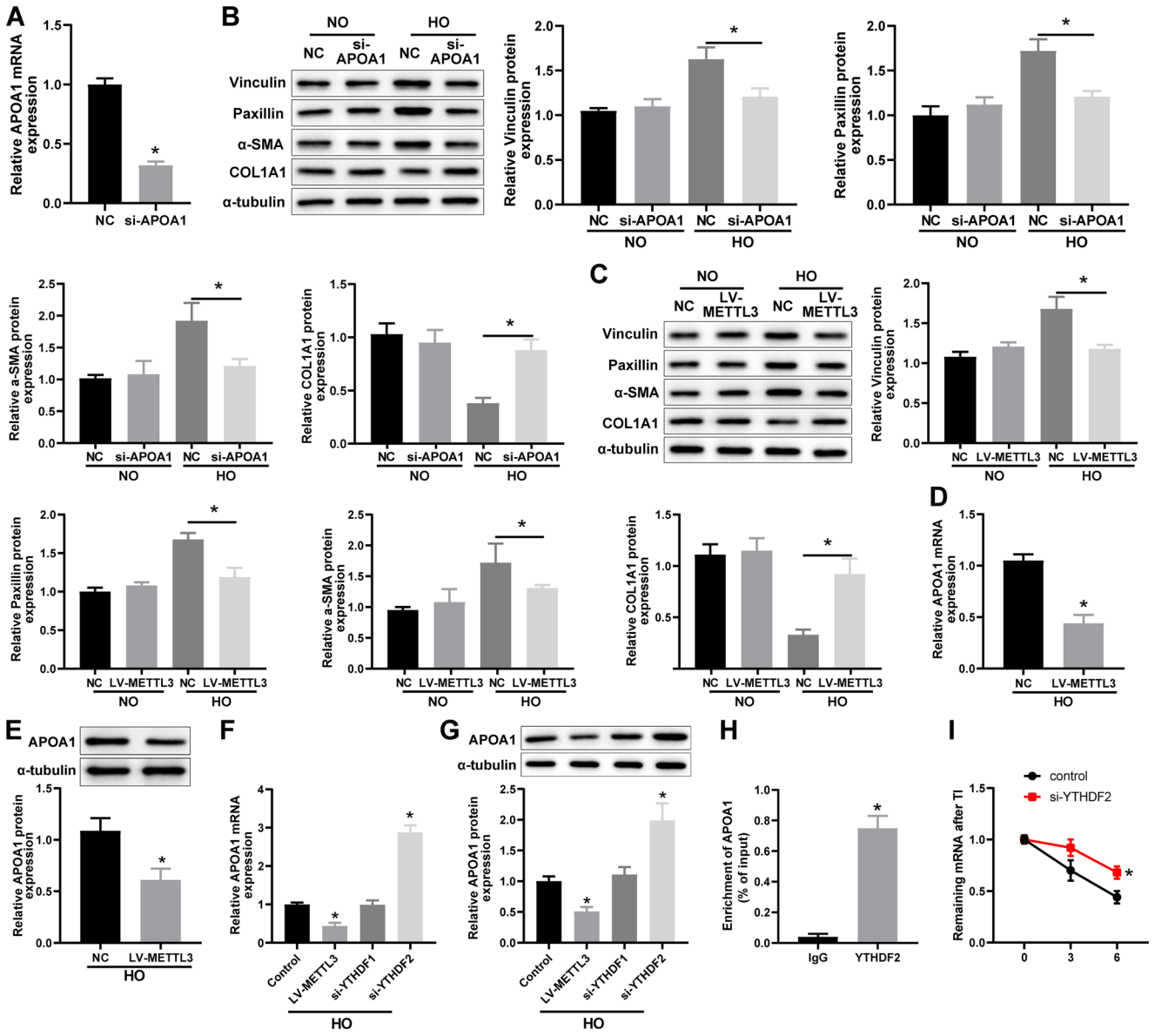

Figure 2. *APOA1* expression was upregulated by *YTHDF2* in hypoxia-treated HSFs. (**A**) RT-qPCR to examine *APOA1* expression with *t*-tests to confirm *P* values. (**B**) Western blotting to evaluate myofibroblast transdifferentiation and collagen production in si-*APOA1*-transfected and hypoxia- or normoxia-treated HSFs. (**C**) Western blotting to evaluate myofibroblast transdifferentiation and collagen production in LV-*METTL3*-transfected and hypoxia- or normoxia-treated HSFs. (**D**, **E**) RT-qPCR (**D**) and western blotting (**E**) to detect APOA1 expression in LV-*METTL3*-transfected and hypoxia-treated HSFs. (**F**, **G**) RT-qPCR (**F**) and western blotting (**G**) to detect APOA1 expression in si-*YTHDF1*- or si-*YTHDF2*-transfected and hypoxia-treated HSFs. (**H**) PAR-CLIP assay to detect the interaction between *YTHDF2* and *APOA1*. (**I**) detection of *APOA1* mRNA degradation rate in si-*YTHDF2*-transfected and hypoxia-treated HSFs. Unless otherwise stated, one-way ANOVA was employed to confirm *P* values with Tukey's multiple comparison tests; $N = 3$.

resulting in 19 differentially expressed genes that interact with *YTHDF2* in myopia. These genes were analyzed for protein interactions using the STRING database (https://cn.string-db.org/) followed by the use of CytoScape software to analyze the degree of interaction, which showed that *FOXM1* had the highest degree of interaction with *METTL3* (Fig. 3A), indicating that *FOXM1* might exert a crucial role in myopia through *METTL3*. GSE136701 microarray analysis indicated that FOXM1 expression was substantially higher in myopic patients compared to controls (Fig. 3B). RT-qPCR and western blotting revealed considerably higher *FOXM1* expression in hypoxia-treated HSFs than in normoxia-treated HSFs (Figs. 3C, 3D). ChIP assays indicated that *FOXM1* was notably enriched in the *METTL3* promoter region in hypoxia-treated HSFs (Fig. 3E). The aforementioned results suggest that *FOXM1* might act in the hypoxia-induced myopic cell model through *METTL3*.

HSFs were then transfected with si-*FOXM1* and treated with hypoxia. RT-qPCR and western blotting results showed that si-*FOXM1* transfection decreased FOXM1 and APOA1 expression and upregulated METTL3 expression (Figs. 3F, 3G). In addition, after si-*FOXM1* transfection, there was no significant change in YTHDF2 expression (Supplementary Fig. S1), which suggested that *APOA1* relied on the m^6A modification of *METTL3* and was recognized by *YTHDF2*, thus affecting the stability of *APOA1*. Furthermore, si-*FOXM1* transfection reversed the hypoxia-induced elevation in vinculin, paxillin, and α-SMA protein levels and

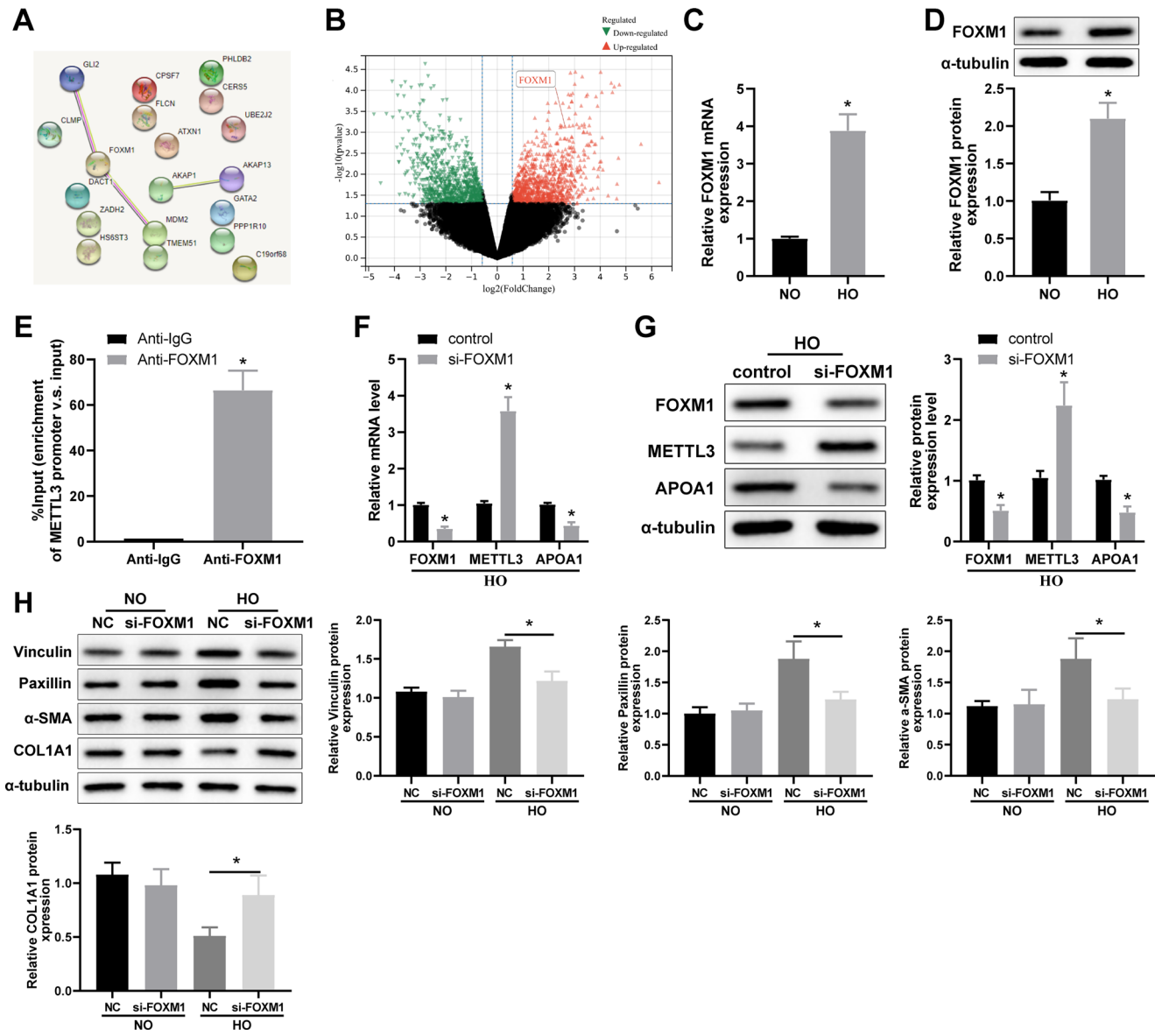

Figure 3. *FOXM1* participates in scleral remodeling in myopia by indirectly affecting *APOA1* expression through inhibition of *METTL3* expression. (**A**) Differentially expressed genes that interact with *METTL3* in myopia were analyzed by the STRING database with CytoScape software to analyze the degree of interaction. (**B**) GSE136701 microarray to analyze *FOXM1* expression in myopia patients. (**C**, **D**) RT-qPCR (**C**) and western blotting (**D**) to detect FOXM1 expression in hypoxia- or normoxia-treated HSFs. (**E**) ChIP assay to evaluate the enrichment level of *FOXM1* in the *METTL3* promoter region. (**F**, **G**) RT-qPCR (**F**) and western blotting (**G**) to detect FOXM1, METTL3, and APOA1 expression in si-*FOXM1*-transfected and hypoxia-treated HSFs. (**H**) Western blotting to assess myofibroblast transdifferentiation and collagen production in si-*FOXM1*-transfected and hypoxia-treated HSFs with one-way ANOVA to confirm *P* values and Tukey's multiple comparison tests. Unless otherwise stated, the *t*-test was applied to confirm the *P* values; $N = 3$.

reduction in COL1A1 protein levels in HSFs (Fig. 3H). These results suggest that *FOXM1* indirectly affects *APOA1* expression by downregulating *METTL3* expression to participate in scleral remodeling in myopia.

Knockdown of *FOXM1* Reverses the Inhibition of Proliferation and Promotion of Apoptosis in HSFs by Hypoxia Treatment Via the *METTL3/APOA1* Axis

Cell proliferation and apoptosis were examined by CCK-8 assay and flow cytometry, which showed that hypoxia treatment inhibited proliferation but promoted apoptosis of HSFs, but these trends were abolished by transfection with si-*FOXM1* (Figs. 4A–4C). In addition, regarding the above indicators, si-*APOA1* or LV-*METTL3* transfection exerted the same effects as si-*FOXM1* transfection (Figs. 4D–4F). These findings indicate that knockdown of *FOXM1* reverses the inhibition of proliferation and promotion of apoptosis in HSFs by hypoxia treatment via the *METTL3/APOA1* axis.

FOXM1 Participates in Scleral Remodeling in Myopia by Regulating *APOA1* Expression Through *METTL3/YTHDF2*

To further confirm whether *FOXM1* affected *APOA1* m^6A methylation levels through *METTL3* and regulated *APOA1* expression by *YTHDF2* specifically recognizing transcripts

Investigative Ophthalmology & Visual Science

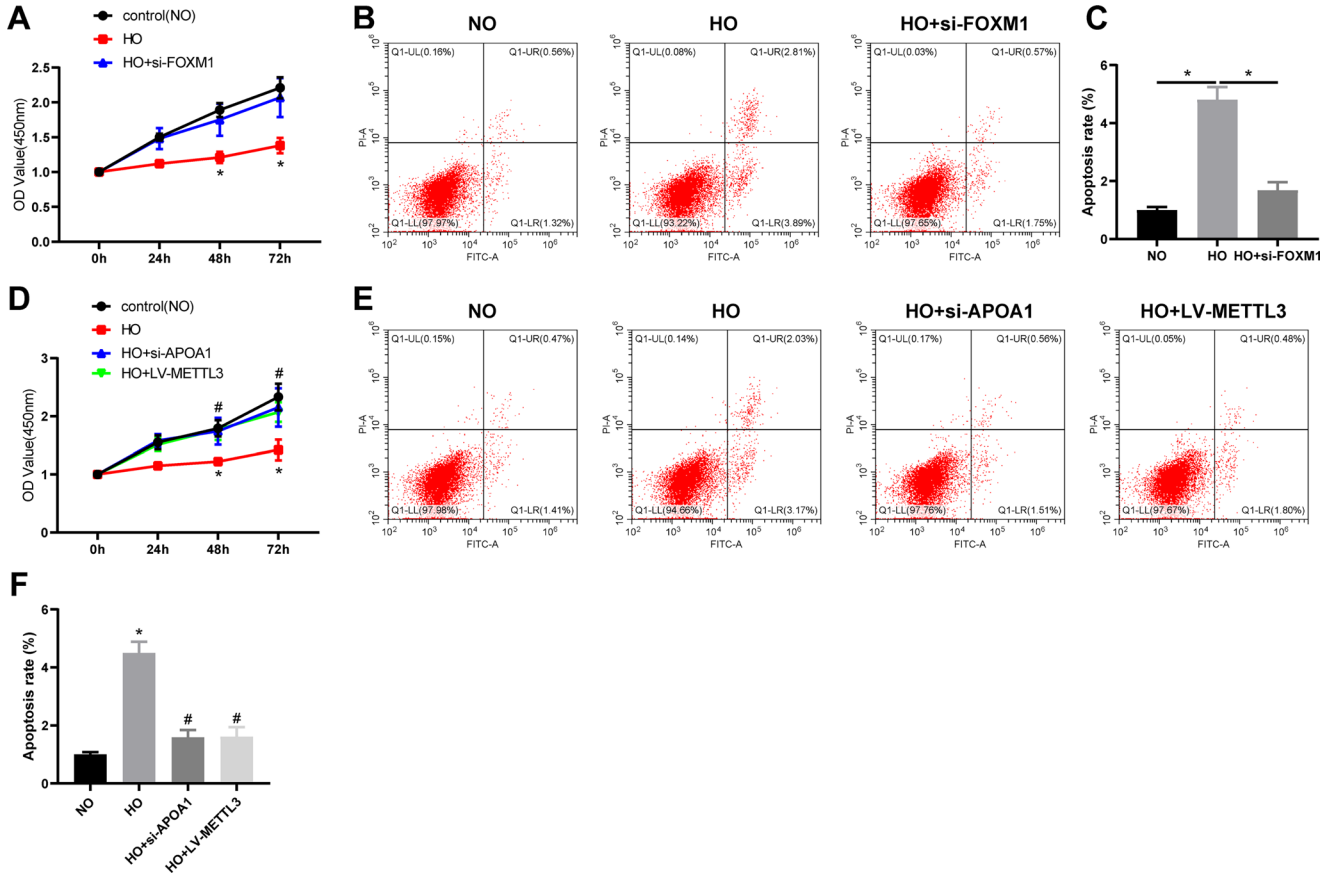

Figure 4. Knockdown of *FOXM1* orchestrated the *METTL3/APOA1* axis to abrogate the influences of hypoxia treatment on proliferation and apoptosis of HSFs. (**A**) CCK-8 assay to determine the proliferation of HSFs treated with normoxia, hypoxia, or hypoxia + si-*FOXM1*, with two-way ANOVA to confirm *P* values. (**B**, **C**) Flow cytometry to determine the apoptosis of HSFs treated with normoxia, hypoxia, or hypoxia + si-*FOXM1*. (**D**) CCK-8 assay to determine the proliferation of HSFs treated with normoxia, hypoxia, or hypoxia + si-*APOA1*, or hypoxia + LV-*METTL3*, with two-way ANOVA to confirm *P* values. (**E**, **F**) Flow cytometry to determine the apoptosis of HSFs treated with normoxia, hypoxia, hypoxia + si-*APOA1*, or hypoxia + LV-*METTL3*. In **C** and **F**, one-way ANOVA was employed to confirm *P* values. The Tukey's test was used for post hoc multiple comparisons for all assays; $N = 3$.

of *APOA1* m^{6}A methylation, thereby affecting scleral remodeling in myopia, HSFs were transfected or cotransfected with si-*FOXM1*, LV-*APOA1*, si-*METTL3*, and si-*YTHDF2* and treated with hypoxia. Western blotting revealed that si-*METTL3*, si-*YTHDF2*, or LV-*APOA1* transfection counteracted the si-*FOXM1* transfection-induced decrease in vinculin, paxillin, and α-SMA protein expression and elevation in COL1A1 protein expression in hypoxia-treated HSFs (Fig. 5A). Moreover, si-*METTL3*, si-*YTHDF2*, or LV-*APOA1* transfection abolished the reduction of apoptosis induced by si-*FOXM1* transfection in hypoxia-treated HSFs (Fig. 5B). A prior study demonstrated that TGF-β1 was one of the cytokines most closely related to the formation of myopia.[21] Therefore, we examined the expression of TGF-β1. Western blotting results revealed that, compared with the NO group, TGF-β1 expression was signally reduced in the HO group, whereas si-*FOXM1* transfection elevated the expression of TGF-β1. Additionally, si-*METTL3*, si-*YTHDF2*, or LV-*APOA1* transfection could reverse the increased effect of si-*FOXM1* on TGF-β1 expression and inhibit the expression of TGF-β1 (Fig. 5C). These results indicated that *FOXM1* elevates the m^{6}A methylation level of *APOA1* by repressing *METTL3* transcription and enhances *APOA1* mRNA stability and transcription by reducing the *YTHDF2*-recognized m^{6}A methylated transcripts, thereby affecting scleral remodeling in myopia by downregulating TGF-β1 expression.

Discussion

Myopia, the most prevalent ocular condition in the world, has become a worldwide public health problem with its increasing prevalence over the last decades.[22] The sclera, a very elastic connective tissue with a complicated structure, accounts for approximately 85% of the outer eyeball tunic and serves crucial roles in vision.[23] The crucial constituents of the sclera are HSFs and the ECM, where the fibroblasts take care of the synthesis of scleral ECM constituents such as collagen, elastic fibers, and proteoglycans.[24,25] Myopia pathogenesis occurs with a transdifferentiation of the cellular phenotype of the sclera from fibroblasts to myofibroblasts and alterations in the ECM.[16] The scleral remodeling performs an essential role in myopia onset and progression and is mainly dependent on variations in the scleral ECM composition, where the accumulation of scleral collagen decreases with myopia progression and the breakdown rises.[26] Hence, it is desirable to expand our understanding of scleral remodeling, which may be beneficial for the understanding of myopia development and myopia

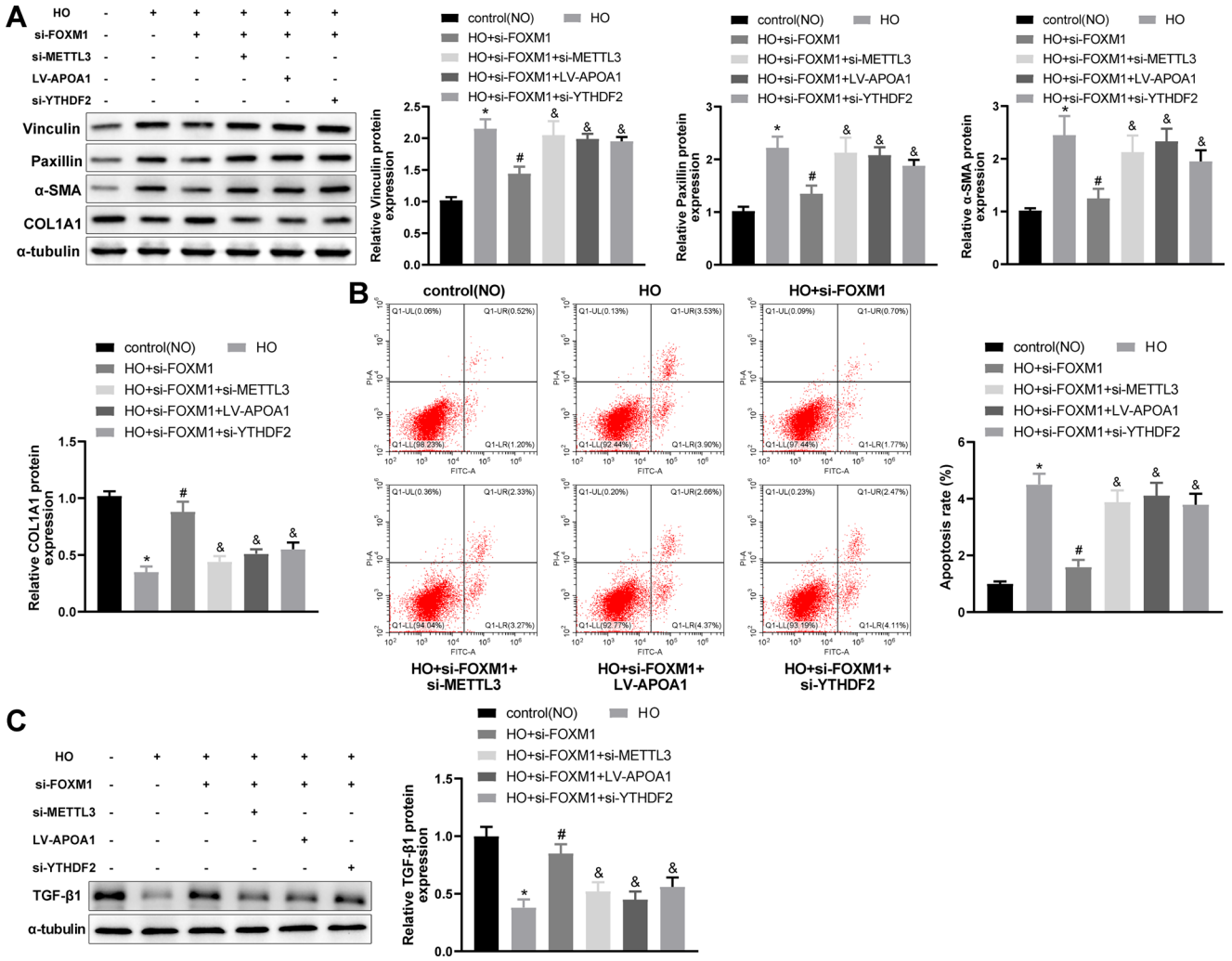

Figure 5. *FOXM1* orchestrated *APOA1* expression through *METTL3/YTHDF2* to participate in scleral remodeling in myopia. (**A**) Western blotting to determine myofibroblast transdifferentiation and collagen production in HSFs. (**B**) Flow cytometry to determine the apoptosis of HSFs. (**C**) Western blotting to determine the protein expression of TGF-β1. One-way ANOVA was employed to confirm *P* values with Tukey's multiple comparison tests; $N = 3$.

management. This study discovered that *FOXM1* participates in scleral remodeling by upregulating *APOA1* expression via *METTL3/YTHDF2*.

Hypoxia in the sclera results in scleral ECM remodeling, which contributes to myopia occurrence.[15] Accordingly, this study employed hypoxia-induced HSFs to construct a myopic cell model. A prior publication illustrated that hypoxic exposure to 5% oxygen facilitated myofibroblast transdifferentiation of HSFs and downregulated type I collagen expression.[16] Fibroblast transdifferentiation generates contractile myofibroblasts that are recognized by particular biomarkers such as vimentin, paxillin, and α-SMA.[27,28] Consistently, the present study also discovered that hypoxia resulted in enhancement in myofibroblast transdifferentiation and diminishment in type I collagen expression as evidenced by upregulation of vinculin, paxillin, and α-SMA protein expression and downregulation of COL1A1 protein expression in HSFs. Moreover, hypoxia treatment inhibited proliferation but promoted apoptosis of HSFs.

APOA1 has beneficial roles in heart, diabetes, atherosclerosis, thrombosis, neurological, and cancer diseases.[29] *APOA1* is differentially expressed in the vitreous and is involved in ocular overgrowth.[30] During the restoration of induced myopia, *APOA1* mRNA and protein expression was remarkably elevated in the choroid of chicks' eyes.[31] Xue et al.[8] stated that *APOA1* was upregulated in patients with pathological myopia and was a potential treatment target for human pathological myopia. In agreement with that study, the present study revealed that *APOA1* was highly expressed in the hypoxia-induced myopic cell model. Moreover, silencing of *APOA1* abrogated the influence of hypoxia on myofibroblast transdifferentiation and type I collagen expression. Database predictions identified multiple m^6A modification sites on APOA1. Correspondingly, this study revealed that the m^6A modification level of *APOA1* was dramatically decreased in the hypoxia-induced myopia model. Of note, *METTL3* and *YTHDF2* were substantially diminished in patients with nuclear cataract and high myopia relative to patients with pure nuclear cataract.[9] The present study observed low expression of *METTL3* in the hypoxia-induced myopia model and inversely targeted *APOA1*. Overexpression of *METTL3*

also reversed the hypoxia-induced elevation in vinculin, paxillin, and α-SMA protein levels and reduction in COL1A1 protein level in HSFs. In addition, knockdown of *YTHDF2* enhanced *APOA1* mRNA and protein expression and slowed down the degradation of *APOA1*. Collectively, the hypoxic myopia model reduced *METTL3* and *YTHDF2*, leading to elevated m^{6}A methylation levels of *APOA1*, reduced recognized m^{6}A methylated transcripts, and enhanced *APOA1* mRNA stability and transcription. Database analysis identified that *FOXM1* was differentially expressed in myopia and could interact with *METTL3*. *FOXM1*, a transcription factor of the conserved FOX family, is a polyfunctional oncoprotein and a potent biomarker for poor prognosis in numerous human neoplasms.[32] A study uncovered that thioredoxin suppresses *FOXM1* and paxillin expression to suppress the metastasis of nasopharyngeal carcinoma cells.[33] In renal interstitial fibrosis, downregulation of *FOXM1* restrains the epithelial-to-mesenchymal transition, as evidenced by decreased α-SMA expression.[34] However, we have found no publications describing the influence of *FOXM1* on ocular diseases. The present study disclosed that *FOXM1* was highly expressed and bound to *METTL3* in the hypoxia-induced myopia model. Silencing of *FOXM1* upregulated *METTL3* to diminish *APOA1* expression. Silencing of APOA1 also counteracted the influence of hypoxia on myofibroblast transdifferentiation, type I collagen expression, proliferation, and apoptosis in HSFs, further reversed by silencing of *METTL3* or *YTHDF2* or overexpression of *APOA1*.

In summary, this work is the first, to the best of our knowledge, to uncover the involvement of *FOXM1* in scleral remodeling in myopia and to find that *FOXM1* restrained myofibroblast transdifferentiation and enhanced type I collagen production in HSF cells by upregulating *APOA1* expression via *METTL3*/*YTHDF2*. However, there are some limitations of our study. First, our study focused only on the mechanism between the *FOXM1*/*METTL3*/*APOA1* axis and its effect on HSF biological phenotypes. It would be more valuable in the future to explore more potential interactions of the *FOXM1*/*METTL3*/*APOA1* axis with other pathways or factors that may affect the remodeling process. Second, our experiments were conducted only at the cellular level. More data and animal studies are needed before the findings of this study can be translated into clinical applications. Overall, this study promises to expand our understanding of myopia and lead to the development of novel ideas for the management of myopia.

Acknowledgments

This research was funded by the grants from Anhui Medical University Research Foundation (grant no. 2023xkj235); Scientific Research Foundation of Anhui Provincial Health Commission (grant no. AHWJ2023A20470) and Key Project of Natural Science in Colleges and Universities of Anhui Province (grant no. 2022AH052324).

Disclosure: **M. Xue**, None; **B. Li**, None; **Y. Lu**, None; **L. Zhang**, None; **B. Yang**, None; **L. Shi**, None

References

1. de Jong P. Myopia: its historical contexts. *Br J Ophthalmol*. 2018;102:1021–1027.
2. Baird PN, Saw SM, Lanca C, et al. Myopia. *Nat Rev Dis Primers*. 2020;6:99.
3. Ikuno Y. Overview of the complications of high myopia. *Retina*. 2017;37:2347–2351.
4. Cooper J, Tkatchenko AV. A review of current concepts of the etiology and treatment of myopia. *Eye Contact Lens*. 2018;44:231–247.
5. Yuan Y, Li M, Chen Q, et al. Crosslinking enzyme lysyl oxidase modulates scleral remodeling in form-deprivation myopia. *Curr Eye Res*. 2018;43:200–207.
6. Xu X, Song Z, Mao B, Xu G. Apolipoprotein A1-related proteins and reverse cholesterol transport in antiatherosclerosis therapy: recent progress and future perspectives. *Cardiovasc Ther*. 2022;2022:4610834.
7. Bertrand E, Fritsch C, Diether S, et al. Identification of apolipoprotein A-I as a "STOP" signal for myopia. *Mol Cell Proteomics*. 2006;5:2158–2166.
8. Xue M, Ke Y, Ren X, et al. Proteomic analysis of aqueous humor in patients with pathologic myopia. *J Proteomics*. 2021;234:104088.
9. Wen K, Zhang Y, Li Y, Wang Q, Sun J. Comprehensive analysis of transcriptome-wide m^{6}A methylome in the anterior capsule of the lens of high myopia patients. *Epigenetics*. 2021;16:955–968.
10. Jiang X, Liu B, Nie Z, et al. The role of m^{6}A modification in the biological functions and diseases. *Signal Transduct Target Ther*. 2021;6:74.
11. Yao MD, Jiang Q, Ma Y, et al. Role of METTL3-dependent N^6-methyladenosine mRNA modification in the promotion of angiogenesis. *Mol Ther*. 2020;28:2191–2202.
12. Yu J, Chai P, Xie M, et al. Histone lactylation drives oncogenesis by facilitating m^{6}A reader protein YTHDF2 expression in ocular melanoma. *Genome Biol*. 2021;22:85.
13. Gartel AL. FOXM1 in cancer: interactions and vulnerabilities. *Cancer Res*. 2017;77:3135–3139.
14. Moose HE, Kelly LE, Nekkalapudi S, El-Hodiri HM. Ocular Forkhead transcription factors: seeing eye to eye. *Int J Dev Biol*. 2009;53:29–36.
15. Zhao F, Zhang D, Zhou Q, et al. Scleral HIF-1α is a prominent regulatory candidate for genetic and environmental interactions in human myopia pathogenesis. *EBioMedicine*. 2020;57:102878.
16. Wu H, Chen W, Zhao F, et al. Scleral hypoxia is a target for myopia control. *Proc Natl Acad Sci USA*. 2018;115:E7091–E7100.
17. Burja B, Kuret T, Janko T, et al. Olive leaf extract attenuates inflammatory activation and DNA damage in human arterial endothelial cells. *Front Cardiovasc Med*. 2019;6:56.
18. Liu J, Eckert MA, Harada BT, et al. m^{6}A mRNA methylation regulates AKT activity to promote the proliferation and tumorigenicity of endometrial cancer. *Nat Cell Biol*. 2018;20:1074–1083.
19. Yang D, Qiao J, Wang G, et al. N^6-Methyladenosine modification of lincRNA 1281 is critically required for mESC differentiation potential. *Nucleic Acids Res*. 2018;46:3906–3920.
20. Vu LP, Pickering BF, Cheng Y, et al. The N^6-methyladenosine (m^{6}A)-forming enzyme METTL3 controls myeloid differentiation of normal hematopoietic and leukemia cells. *Nat Med*. 2017;23:1369–1376.
21. Zhu X, Du Y, Li D, et al. Aberrant TGF-β1 signaling activation by MAF underlies pathological lens growth in high myopia. *Nat Commun*. 2021;12:2102.
22. Wang WY, Chen C, Chang J, et al. Pharmacotherapeutic candidates for myopia: a review. *Biomed Pharmacother*. 2021;133:111092.
23. Boote C, Sigal IA, Grytz R, Hua Y, Nguyen TD, Girard MJA. Scleral structure and biomechanics. *Prog Retin Eye Res*. 2020;74:100773.
24. Hu D, Jiang J, Ding B, Xue K, Sun X, Qian S. Mechanical strain regulates myofibroblast differentiation of human scleral fibroblasts by YAP. *Front Physiol*. 2021;12:712509.

25. Atta G, Schroedl F, Kaser-Eichberger A, et al. Scleraxis expressing scleral cells respond to inflammatory stimulation. *Histochem Cell Biol*. 2021;156:123–132.
26. Yu Q, Zhou JB. Scleral remodeling in myopia development. *Int J Ophthalmol*. 2022;15:510–514.
27. Matthijs Blankesteijn W. Has the search for a marker of activated fibroblasts finally come to an end? *J Mol Cell Cardiol*. 2015;88:120–123.
28. Li Y, Tang CB, Kilian KA. Matrix mechanics influence fibroblast-myofibroblast transition by directing the localization of histone deacetylase 4. *Cell Mol Bioeng*. 2017;10:405–415.
29. Cochran BJ, Ong KL, Manandhar B, Rye KA. APOA1: a protein with multiple therapeutic functions. *Curr Atheroscler Rep*. 2021;23:11.
30. Yu FJ, Lam TC, Liu LQ, et al. Isotope-coded protein label based quantitative proteomic analysis reveals significant up-regulation of apolipoprotein A1 and ovotransferrin in the myopic chick vitreous. *Sci Rep*. 2017;7:12649.
31. Summers JA, Harper AR, Feasley CL, et al. Identification of apolipoprotein A-I as a retinoic acid-binding protein in the eye. *J Biol Chem*. 2016;291:18991–19005.
32. Liu C, Barger CJ, Karpf AR. FOXM1: a multifunctional oncoprotein and emerging therapeutic target in ovarian cancer. *Cancers (Basel)*. 2021;13:3065.
33. Jiang L, Wang P, Chen H. Overexpression of FOXM1 is associated with metastases of nasopharyngeal carcinoma. *Ups J Med Sci*. 2014;119:324–332.
34. Wang Y, Zhou Q, Tang R, Huang Y, He T. FoxM1 inhibition ameliorates renal interstitial fibrosis by decreasing extracellular matrix and epithelial-mesenchymal transition. *J Pharmacol Sci*. 2020;143:281–289.

Investigative Ophthalmology & Visual Science